general design concept for tandem solar cells. For this reason, we use typical refractive index values for the different layers, rather than detailed experimental dispersion data.

The bottom cell model is based on the 25% efficient c-Si PERL cell reported in [24, 25]. The response of this cell is calculated in two steps. First, the light transmitted through the top cell is calculated by including a semi-infinite Si substrate in the transfer matrix calculations described above. The transmitted spectrum is then combined with the measured external quantum efficiency (EQE) of the PERL cell [24, 26] to estimate the absorption and corresponding short circuit current. Thus, the bottom cell absorption curves shown in Fig. 2(a) are the experimental EQE curves modulated by the transmission spectrum of the top cell and intermediate layers.

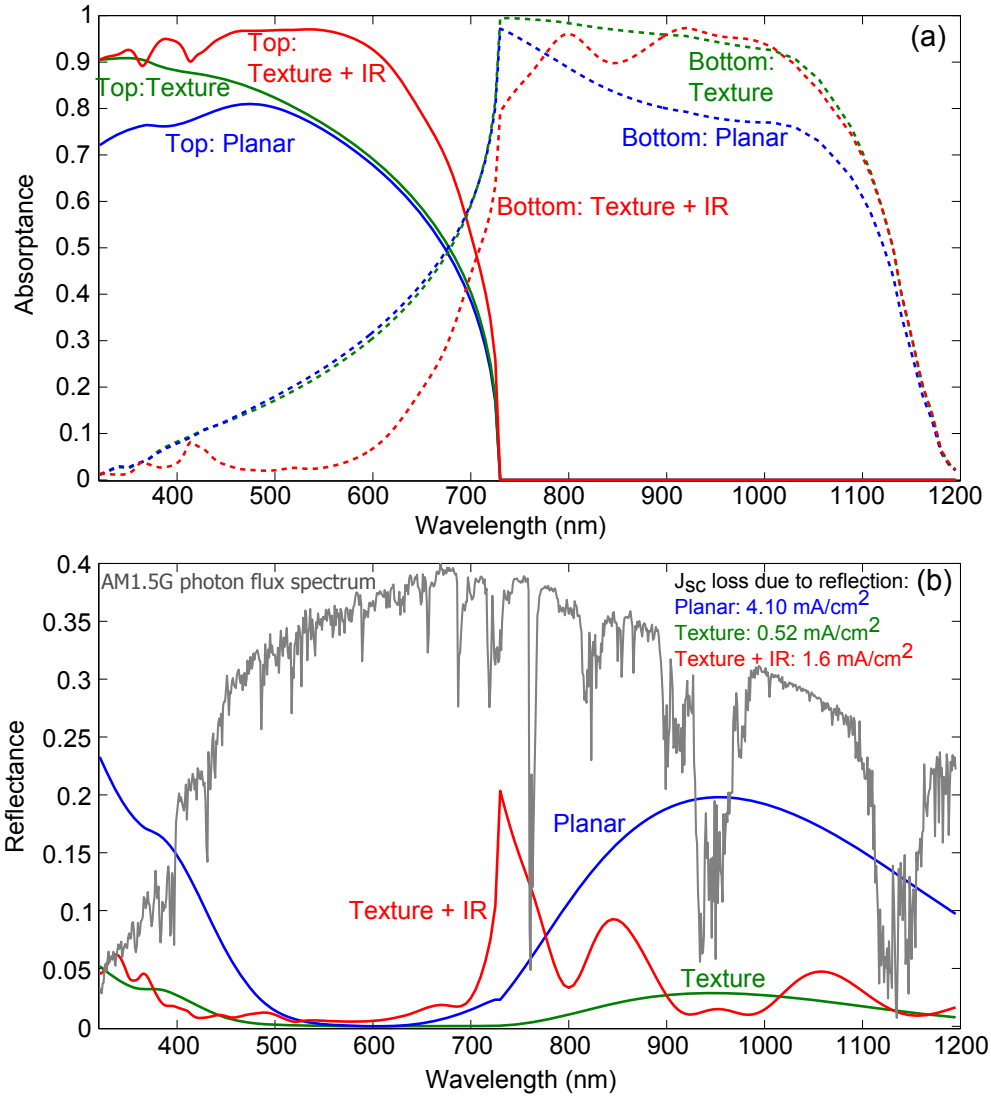

Fig. 2. Reflectance and absorptance in the top and bottom cells for various cell structures vs. wavelength. All structures have a thickness-optimized SLARC and top cell thickness of 150 nm. (a) Absorptance in top and bottom cells. (b) Front-surface reflectance and equivalent reflected J_{sc} values for each structure. A normalized AM1.5G solar spectrum is overlaid in gray for reference.

#216827 - $15.00 USD Received 11 Jul 2014; revised 4 Aug 2014; accepted 17 Aug 2014; published 28 Aug 2014

4. Results

As a reference case, we first consider an all-planar tandem cell with a SLARC on the front and no intermediate reflector. Throughout this paper the ARC film is taken to be a lossless dielectric with a refractive index of 1.7 (similar to Al_2O_3), with the thickness optimized to give the best tandem cell efficiency for each structure. The corresponding absorption and reflection spectra for a planar 150 nm thick perovskite top cell are plotted as blue curves in Fig. 2. Comparing the curves in Fig. 2(a) and 2(b) shows that the planar top cell suffers from reflection loss at short wavelengths ($\lambda < 500\,\text{nm}$), and weak absorption at wavelengths $500\,\text{nm} < \lambda < 730\,\text{nm}$ while the planar Si bottom cell suffers significant reflection losses at wavelengths $\lambda > 800\,\text{nm}$. The integrated reflection loss for the planar cell is equivalent to a short current loss of $4.1\,\text{mA}\,\text{cm}^{-2}$ under AM1.5G illumination.

To reduce the reflection losses, we next consider a textured cell structure as shown in Fig. 1, but without the intermediate reflector layer (green curves in Fig. 2). We assume that the front surface of the Si cell is patterned with inverted pyramids, and the thin top cell and optimized SLARC are deposited conformally over the surface. Pyramidal surface textures (upright and inverted) are commonly used on monocrystalline silicon cells for antireflection and light-trapping. The typical feature size is $2\,\mu\text{m} - 10\,\mu\text{m}$ and thus they can be modelled accurately using ray-optics [8]. Here we assume an inverted pyramid texture as illustrated in Fig. 1, but similar results would be expected for upright pyramids. In the ray optics regime there is no direct coupling of light between inverted pyramids, so random and regular arrays have the same optical response. We apply the semi-analytic approach of [8, 27], taking into account the multiple ray paths illustrated in Fig. 1(b). This method requires as inputs only the angle-dependent reflection and transmission coefficients of a single planar facet. Note that we correct the path proportions from those errantly reported in [8], so that 40% of incident light follows path B (Fig. 1(b)). As expected, the textured surface reduces the reflectance dramatically across the whole wavelength range of interest, resulting in an integrated reflection loss equivalent to $0.52\,\text{mA}\,\text{cm}^{-2}$ – almost eight times lower than the planar reference.

Despite the excellent anti-reflection provided by the surface texture, it offers no significant light trapping in the top cell. This can be seen by comparing the top cell absorption curves for the planar (blue) and textured (green) cells in Fig. 2(a). At wavelengths below 730 nm, absorption in the bottom cell is almost identical for the planar and simple textured cell structures, with $\sim 25\%$ of photons with energy $hc/\lambda > 1.7\,\text{eV}$ absorbed by the Si. Ideally, all such high-energy photons would be absorbed in the top cell to gain the maximum benefit of the larger bandgap. This requires wavelength-selective light trapping to increase absorption of short wavelength light in the top cell while transmitting long wavelength light to the bottom cell.

To provide light trapping in the top cell we next consider the addition of a wavelength-selective intermediate reflector (IR) between the top and bottom cells as shown in Fig. 1. The purpose of the IR is to prevent short wavelength light from entering the Si cell by reflecting it back through the top cell, as shown in Fig. 1(c). The path length enhancement in the top cell can therefore be up to a factor of four or six, depending on which of the ray paths in Fig. 1(b) the light follows. We choose a basic Bragg stack reflector consisting of alternating TiO_2 ($n_H = 2.4$) and SiO_2 ($n_L = 1.46$) layers with relative thicknesses fixed to maintain an equal optical path length in each material. A stack of four n_H/n_L layer pairs was chosen to ensure very high reflectance at the desired wavelengths, however we have found that fewer layers can provide relatively good light trapping, which may be desirable to simplify fabrication. Following the approach in [28], an additional thin (half-layer) SiO_2 film is included on the front and back of the stack to maximize coupling in and out of the IR layer, thereby minimizing reflectance at longer wavelengths.

Although it is straightforward to design a Bragg stack to achieve a reflectance band at a

#216827 - $15.00 USD Received 11 Jul 2014; revised 4 Aug 2014; accepted 17 Aug 2014; published 28 Aug 2014

specific wavelength for one angle of incidence, it is nontrivial to design one for the textured surface in Fig. 1, where light undergoes multiple reflections. The design process is further complicated by the requirement to minimize reflectance for longer wavelengths. For this reason we perform a simple numerical optimization of the IR layer thickness and the SLARC thickness in order to maximize the overall tandem efficiency (calculated as in Sec. 5). The optimization is repeated for each top cell thickness.

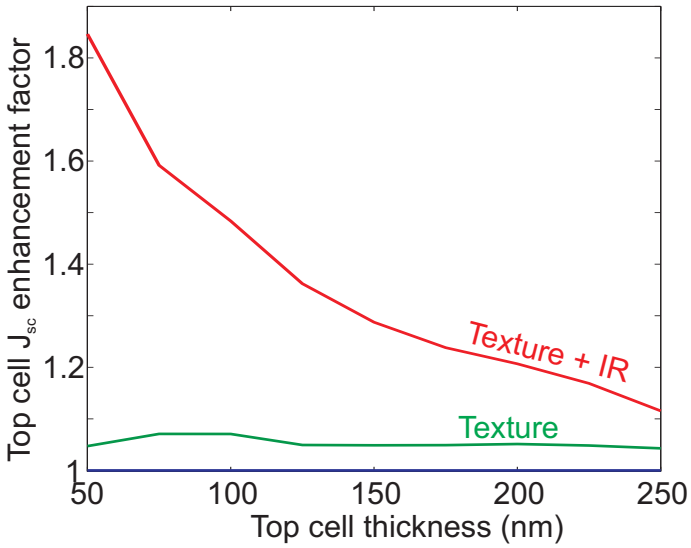

Fig. 3. J_{sc} enhancement factor for each cell structure vs. top cell thickness. This factor is the ratio of the top cell J_{sc} of a given structure to the J_{sc} of the planar cell at equal top cell thickness

The red curves in Fig. 2(a) show the absorptance in the top and bottom cells with the optimized texture/IR combination for a 150 nm thick top cell. The corresponding reflectance spectrum is plotted in Fig. 2(b). Light trapping of short wavelength light is evident by the increased absorption in the top cell and corresponding decrease in absorption in the bottom cell. Less than 12% of photons with energy $hc/\lambda > 1.7$ eV are absorbed in the bottom cell, while the overall reflectance remains $< 5\%$ at these wavelengths. Figure 2(b) shows a slight increase in reflectance with the addition of the IR layer, resulting in an integrated reflection loss of $1.6\,\mathrm{mA\,cm^{-2}}$. Most of this increase is due to imperfect transmission of long wavelength light through the IR layer, which could perhaps be improved with a more complex IR design.

Figure 3 shows the relative current enhancement in the top cell as a function of its thickness for the texture-only and texture/IR cases, normalized to the planar reference structure. The texturing alone achieves a current increase of $\approx 5\%$ for all top cell thicknesses, indicating reduced reflectance, but little light trapping. In contrast, adding the wavelength-selective IR layer between the cells increases current in the top cell by $> 80\%$ for a 50 nm thick top cell, and $\sim 11\%$ for a 250 nm thick cell. The large enhancement for thin films, and strong dependence on cell thickness is characteristic of effective light trapping in the top cell. Thus, the proposed tandem cell geometry in Fig. 1 successfully combines the excellent broadband anti-reflection properties of conventional pyramidal surface texturing with wavelength-selective light trapping in the thin-film top cell.

Although the results presented so far demonstrate reduced reflectance and improved light trapping in the top cell, further analysis is required to understand the potential efficiency gains

#216827 - $15.00 USD Received 11 Jul 2014; revised 4 Aug 2014; accepted 17 Aug 2014; published 28 Aug 2014

offered by this approach. In the next section we use a simple tandem cell efficiency model reported in [6] to estimate the overall tandem cell efficiency.

5. Tandem cell efficiency

In this section we follow the approach described in [6] to calculate the efficiency of a 4-terminal tandem cell using the calculated absoption spectra in Fig. 2. In this model, the carrier collection and voltage properties of the top cell depend on the cell thickness, and are characterized by the bandgap ($E_{g,top} = 1.7\,\mathrm{eV}$), carrier diffusion length ($L_d = 110\,\mathrm{nm}$), and luminescence efficiency $\Phi = 0.55$ of the absorbing layer. The chosen values of L_d and Φ are based on experimentally-determined values for solution-processed perovskite films reported in [4] and [29] respectively. As in [6], here we assume the top cell has a fill-factor of 0.8, which, while higher than current perovskite cells, is a realistic target for future high efficiency devices.

Carrier collection in the Si bottom cell is already accounted for in the absorption data (Fig. 2) where we used the experimental EQE curves for a high efficiency PERL cell, as described in Sec. 3. A simple one-diode model is then used to calculate the V_{oc} of the bottom cell as a function of the calculated J_{sc}. We assume that the fill-factor and J_0 are unchanged from their values under standard test conditions.

With the above models for the top and bottom cell performance, the total output power of the 4-terminal device is given by $P = FF^{(1)}V_{oc}^{(1)}J_{sc}^{(1)} + FF^{(2)}V_{oc}^{(2)}J_{sc}^{(2)}$, where the superscripts 1 and 2 denote the top cell and bottom cell respectively [6].

Figure 4 shows the short circuit current density in the top and bottom cells (a) and the calculated tandem cell efficiency (b) as a function of top cell thickness for the three cases studied here: the planar reference cell; the textured cell; and the textured cell with intermediate reflector. As seen in Fig. 4(a), the surface texture provides an almost fixed increase in the top cell J_{sc} of $\sim 5\%$, and a relatively larger increase in the bottom cell J_{sc}, resulting in an absolute efficiency increase of $\sim 2\%$ for most cell thicknesses (Fig. 4(b)). Comparing the reflectance curves in Fig. 2(b) for the planar and textured cases, it is clear that this increase is largely due to reduced front surface reflectance at wavelengths above 730 nm.

Despite a small increase in reflection loss ($\sim 1.1\,\mathrm{mA\,cm^{-2}}$), the addition of the IR achieves further absolute efficiency gains of $1-2\%$ above those of the basic textured cell, and $2-4\%$ above the planar reference cell. This is due to the large top cell J_{sc} enhancement resulting from effective light-trapping of short wavelength light (Fig. 2). This transfer of current to the top cell results in a net efficiency gain due to its higher V_{oc}.

Figure 4(b) also shows the efficiency beginning to saturate for top cell thicknesses of 250 nm for the optimized texture + IR structure. This is a result of almost complete absorption of above-bandgap light in the top cell. Further increase in cell thickness eventually results in decreasing current and overall efficiency due to reduced collection efficiency (noting that the carrier diffusion length considered here was 110 nm).

Light trapping also has the effect of bringing the top and bottom J_{sc} values closer to each other: the difference between top and bottom J_{sc} for the cell with the IR is $< 5\,\mathrm{mA\,cm^{-2}}$ for a 150 nm thick top cell, compared to $> 12\,\mathrm{mA\,cm^{-2}}$ for the simple textured cell (see Fig. 4(a)). Hence, the light trapping scheme proposed here could also provide effective photon management in series connected cells where current-matching is required.

6. Conclusion

We present a practical tandem cell structure combining conventional pyramidal surface texturing on the Si bottom cell with a wavelength-selective intermediate reflector. This design satisfies the three optical requirements for high-performance perovskite-on-silicon tandem solar cells: low front surface reflectance, light-trapping of short wavelength light, and high transmission of

#216827 - $15.00 USD Received 11 Jul 2014; revised 4 Aug 2014; accepted 17 Aug 2014; published 28 Aug 2014

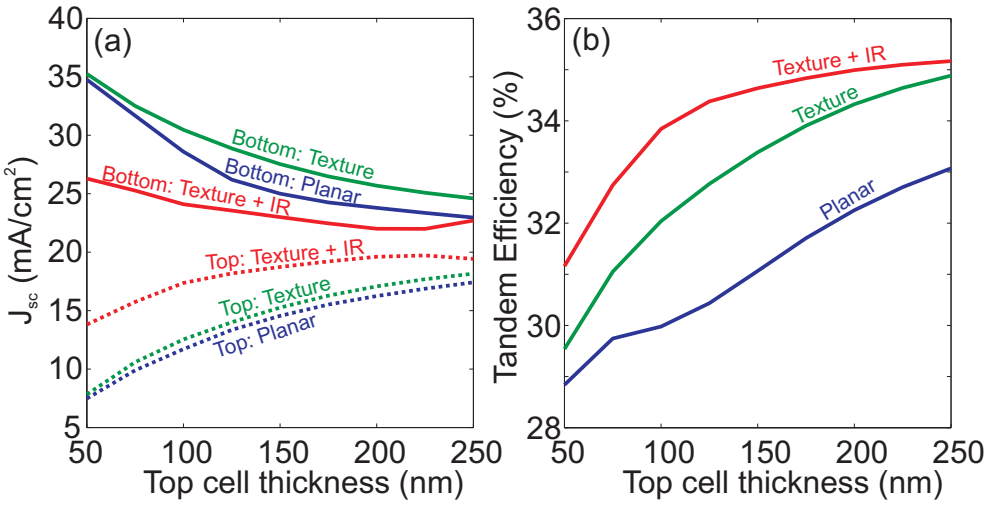

Fig. 4. (a) Jsc for top and bottom cells for each structure vs. top cell thickness. (b) Efficiency of each structure vs. top cell thickness.

long wavelength light to the bottom cell. We calculate front-surface reflection losses as low as $1.6\,\mathrm{mA\,cm^{-2}}$, and top cell current enhancements of $>80\%$ for a 50 nm thick perovskite top cell, and $>20\%$ for a 200 nm top cell. This performance corresponds to absolute efficiency increases of $2-4\%$ compared to a planar tandem cell with a single layer ARC on the front surface. Using a simple tandem cell efficiency model, we have shown that efficiencies as high as 35% may be achievable with an optimal high-bandgap perovskite top cell.

While the concept has been demonstrated for a specific tandem cell combination, it is applicable to any thin-film on Si tandem cell provided a high quality top cell can be fabricated conformally on the textured bottom cell. This has been recently demonstrated for a-Si cells [12], and is well-suited to evaporated perovskite cells [5]. We would also expect similar performance enhancements on other Si surface textures such as upright and random pyramids.

This work shows that existing high-efficiency front-surface textured c-Si cell designs offer an ideal substrate to deposit a thin film top cell. The approach is therefore directly compatible with mechanically-stacked tandem cells with little or no modification to the Si cell manufacturing process, and is therefore highly attractive for rapid development of silicon-based tandems. Such integrated light trapping will also be important for series-connected tandem cells where high absorption in the top cell is crucial for current matching requirements.

Acknowledgment

N.N.L is supported by an Australian Renewable Energy Agency (ARENA) postdoctoral fellowship.

#216827 - $15.00 USD Received 11 Jul 2014; revised 4 Aug 2014; accepted 17 Aug 2014; published 28 Aug 2014